ELSEVIER

Catalysis Today 44 (1998) 223–233

CATALYSIS TODAY

Transalkylation of toluene and 1,2,4-trimethylbenzene over large pore zeolites

Yong-Kul Lee, Se-Ho Park, Hyun-Ku Rhee*

Department of Chemical Engineering, Seoul National University, Kwanak-ku, Seoul 151-742, South Korea

Abstract

Large pore zeolites, H-beta, H-mordenite (H-MOR) and H-omega, were dealuminated by steam treatment followed by acid leaching and were applied for transalkylation of toluene and 1,2,4-trimethylbenzene. The acidic properties of catalysts were examined by using TPD of ammonia and in situ FT-IR spectroscopy in the OH stretching region as well as pyridine adsorbed catalysts. XRD, mid-infrared spectroscopy and ^{29}Si and ^{27}Al MAS-NMR techniques were employed to investigate the structural changes of zeolites during dealumination process. Among the parent zeolites, H-beta and H-MOR showed high activity for transalkylation. H-omega showed very low activity although its acidity turned out to be high compared to that of H-MOR or H-beta. Over dealuminated samples, the activity was in the order H-MOR>H-omega≈H-beta unlike over the parent zeolites. It was observed that a large number of Brønsted acid sites were present in small pores and cages in H-MOR and H-omega. After dealumination, the activity and stability were substantially improved for H-MOR and H-omega but decreased for H-beta. H-MOR and H-omega tended to have more open structure and some of occluded acid sites became exposed to the main channels of 12-MR by dealumination. Such structural changes are believed to compensate for the loss of total acid sites to bring about the enhanced activity and stability over H-MOR and H-omega. Dealuminated H-omega, however, was deactivated rather rapidly. Consequently, H-MOR could be considered as a good acid catalyst for transalkylation of toluene and 1,2,4-trimethylbenzene after treatment by steam followed by acid leaching.

Keywords: H-beta; H-mordenite; H-omega; Transalkylation; Dealumination

1. Introduction

Transalkylation of toluene and C_9 aromatics has attracted considerable attention because this reaction leads to the production of xylene, which is an important starting material for the production of synthetic fibers, plasticizers and resins [1]. Zeolite catalysts such as mordenite, Y zeolite and zeolite beta have been reported to be effective in transalkylation of toluene and C_9 aromatics [1–5]. Meshram et al. [6] found that C_9 aromatics could not diffuse effectively into the inner channels of ZSM-5 having 10-MR pore openings, thus zeolites with large pore size of 12-MR pore openings are needed for this reaction.

According to the previous studies [1–5], the acidity of zeolites is another important factor. The higher the acidity of the zeolites, the better the activity becomes.

*Corresponding author. Tel.: +82 2 880 7405; fax: +82 2 880 7295; e-mail: hkrhee@plaza.snu.ac.kr

0920-5861/98/$32.00
PII S0920-5861(98)00194-1

Zeolite catalysts, however, exhibit deactivation problem caused by coke deposition in the zeolite channels and thus the durability of zeolite against coking should be enhanced for the commercial application. Dealumination by steam and acid treatment is a useful method for the enhancement of the catalytic stability and its application to zeolites for various reactions has been reported in [7–10].

In the present study, we investigated the catalytic activities of H-mordenite, H-beta and H-omega, which have 12-MR pore openings, and of their dealuminated samples. We also examined the physicochemical properties of catalysts by various characterization techniques and the effects of dealumination on the activity and stability of the zeolites for transalkylation of toluene and 1,2,4-trimethylbenzene (TMB). In commercial processes such as BTX units, trimethylbenzene isomers are the major components in C_9 aromatics and the fraction of 1,2,4-TMB among three isomers is about 65% [4]. For this reason, toluene and 1,2,4-TMB were used as the reactants.

2. Experimental

2.1. Catalysts preparation

H-beta (SiO_2/Al_2O_3=25 and 75, PQ) and H-mordenite (SiO_2/Al_2O_3=45, Engelhard) used in this study were taken from commercial samples. Zeolite omega was synthesized hydrothermally by separate nucleation and growth steps according to the procedure reported by Figueras and co-workers [11]. The XRD pattern of synthesized omega matched well with that reported earlier [11]. The as-synthesized zeolite omega was transformed into the ammonium form by ion-exchange with 1 M NH_4Cl solution at 80°C for 12 h which was repeated three times. It was then calcined in air at 600°C for 5 h to yield H-omega.

The dealuminated zeolites were prepared by steaming the H-form zeolites at various temperatures in a fixed-bed flow reactor with a specific partial pressure of steam and by subsequent acid leaching treatment in 0.05 N HNO_3 solution under reflux condition at 80°C for 8 h. After dealumination, the samples were calcined in air at 500°C for 5 h.

The Si/Al ratio of zeolites was determined by energy dispersive X-ray (EDX) and induced coupled plasma (ICP). The crystallinity was examined by X-ray powder diffraction (XRD). The catalysts examined in this study are summarized with dealumination conditions in Table 1.

2.2. Catalysts characterization

2.2.1. Ammonia TPD

To examine the acidities of catalysts, temperature programmed desorption of ammonia was performed under He flow. The sample of 0.1 g was pretreated at 500°C for 1 h, cooled down to 100°C and then satu-

Table 1
Parent and dealuminated zeolites examined in this study and dealumination conditions

Parent samples	Dealuminated samples	Si/Al[a]	Steaming conditions		
			Pressure (P_{H_2O}, kPa)	Temperature (°C)	Duration (h)
H-MOR (Si/Al=22.5)	$MSA_{500,0.5}$	29.5	13.8	500	0.5
	$MSA_{600,2}$	37.6	13.8	600	2
	$MSA_{700,2}$	38.5	13.8	700	2
	$MSA_{700,4}$	45.6	24.3	700	4
H-beta(12.5)	$BSA_{500,2}$	—	13.8	500	2
H-beta(37.5)	$BSA_{500,2}$	—	13.8	500	2
H-omega(5.6)	$OMSA_{600,2}$	11.2	37.1	600	2
	$OMSA_{700,2}$	—	37.1	700	2
	$OMSA_{700,2}$[b]	29.5	37.1	700	2
	$OMSA_{700,4}$	—	37.1	700	4

[a] Determined by EDX.
[b] Acid leaching in 0.1 N HNO_3 solution.

rated with ammonia. The TPD was started by increasing temperature at a rate of 10°C/min.

2.2.2. FT-IR studies

Infrared spectra were recorded on a Nicolet Impact 410 instrument with a resolution of 4 cm^{-1}. To obtain mid-infrared spectra, the sample was dispersed in KBr (sample/KBr=1/50 weight ratio) and pressed to wafer (40 mg). The spectra in the framework region (1500–400 cm^{-1}) were taken at room temperature. For FT-IR study of hydroxyl groups and pyridine adsorbed catalysts, self-supporting wafers (13 mg) were activated in situ under He flow at 500°C for 1 h. The IR spectra of parent catalysts in OH stretching region were obtained under He flow in a glass cell which was equipped with NaCl windows and high-vacuum stopcocks. Afterwards, the glass cell was evacuated to a pressure of approximately 10^{-2}–10^{-3} Torr. After pyridine (3 Torr) was introduced at 100°C for 15 min, the cell was sufficiently evacuated to eliminate physisorbed species. The spectra were obtained at various temperatures.

2.2.3. MAS NMR spectroscopy

To investigate the structural changes caused by dealumination, the ^{29}Si and ^{27}Al MAS NMR spectra were recorded on a Bruker AM-300 NMR spectrometer. The ^{29}Si and ^{27}Al spectra were measured at 59.631 and 78.206 MHz, respectively, with the same spinning frequency of 4 kHz. Chemical shifts of ^{29}Si spectra were referenced to tetramethylsilane, and that of ^{27}Al spectra were given in ppm from $Al(H_2O)_6^{3+}$.

2.3. Reaction experiment

Reactions were conducted in a fixed-bed flow reactor at 400°C with WHSV=2.8 h^{-1} and He/feed molar ratio of 12.0. Catalysts were activated in He flow at 500°C for 30 min and then cooled down to the reaction temperature. Mixture of toluene and 1,2,4-TMB with one-to-one molar ratio was fed to the reactor by a microfeeder. Reaction products were collected and analyzed with an HP 5890 gas chromatograph equipped with FID. The capillary column, HP-1 (25 m, 0.17 μm, 0.32 mm ID), was used.

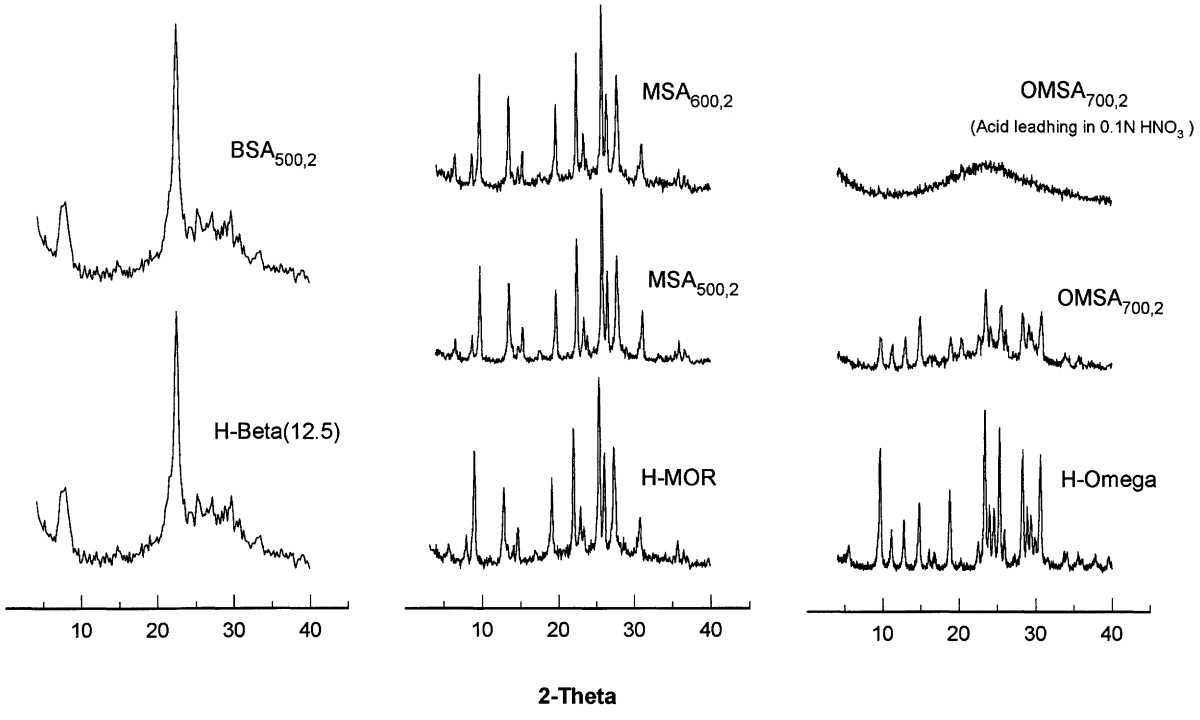

Fig. 1. XRD patterns of parent and dealuminated zeolites.

3. Results and discussion

3.1. Catalysts characterization

3.1.1. XRD crystallinity

Dealumination by steam treatment followed by acid leaching caused no significant loss of crystallinity of H-beta and H-MOR. Miller et al. [12] has reported that in mordenite, aluminum vacant sites formed by steam treatment was replaced by neighboring silicon atoms and this brought about more stabilized structure. This feature was also observed in our XRD results for H-beta and H-MOR, but not for H-omega. Crystallinity of H-omega decreased considerably with the degree of acid leaching as shown in Fig. 1.

3.1.2. ^{29}Si MAS NMR

The ^{29}Si MAS NMR spectra of H-MOR and of its dealuminated samples are presented in Fig. 2. Peaks

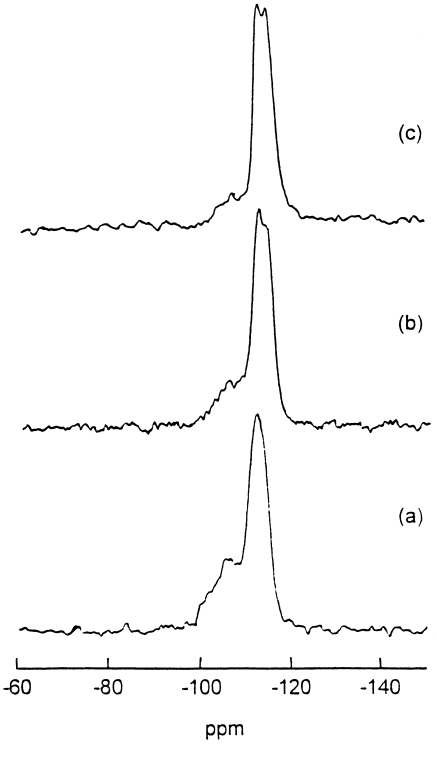

Fig. 2. ^{29}Si MAS NMR spectra of (a) H-MOR, (b) $MSA_{500,2}$, and (c) $MSA_{600,2}$.

for Si(0Al) at −112 ppm and Si(1Al) at −105 ppm, and a small shoulder at −98 ppm for Si(2Al) were observed [13]. With the degree of dealumination, peak intensities corresponding to Si(1Al) and Si(2Al) decreased. In addition, splitting of the peak at −110 ppm was induced. This indicates that dealumination was progressed rather severely. Mordenite has crystallographically four nonequivalent tetrahedral sites (T_1:T_2:T_3:T_4=2:2:1:1) [14], so the peak at −110 ppm is practically composed of peaks related to four different tetrahedral sites. These peaks are separated clearly in more silicious environments [13].

Zeolite omega has 24 tetrahedral sites per unit cell located in the four-membered rings in the gmelinite cages (A sites) and 12 sites per unit cell located in the six-membered rings through which the gmelinite cages are linked in parallel to the screw axis (B sites) [15]. Therefore, the ^{29}Si MAS NMR spectrum of zeolite omega is composed of two mutually overlapping families of signals due to the presence of two kinds of crystallographically nonequivalent silicon atoms. The spectra for each type of sites have been assigned as SiA(2Al) at −94.8 ppm, Si_A(1Al) at −100.2 ppm, Si_A(0Al) at −105.7 ppm, Si_B(2Al) at −102.3 ppm, SiB(1Al) at −107.7 ppm and Si_B(0Al) at −113 ppm [16].

In our study, the ^{29}Si MAS NMR spectrum of H-omega, as shown in Fig. 3, consists of two broad peaks and two shoulders with half-intensity corresponding to Si_A(2Al) at −94.7 ppm, Si_A(1Al) at −100.6 ppm, Si_A(0Al) at −105.8 ppm and Si_B(0Al) at −114.7 ppm, respectively. After dealumination, a partial resolution peak at −107.5 ppm corresponding to Si_B(1Al) site was observed. However, the intensity of this peak was very weak and slightly affected by dealumination, whereas those of Si_A(2Al) and Si_A(1Al) decreased considerably. This result indicates that most of the aluminum species exist in S4R of gmelinite cage and are removed preferentially by dealumination.

3.1.3. ^{27}Al MAS NMR

As shown in Fig. 4, the ^{27}Al MAS NMR spectrum of H-MOR consists of one sharp resonance at 55 ppm which is assigned to structural, tetrahedral aluminum and another small resonance at 0 ppm which is assigned to nonstructural, octahedral aluminum

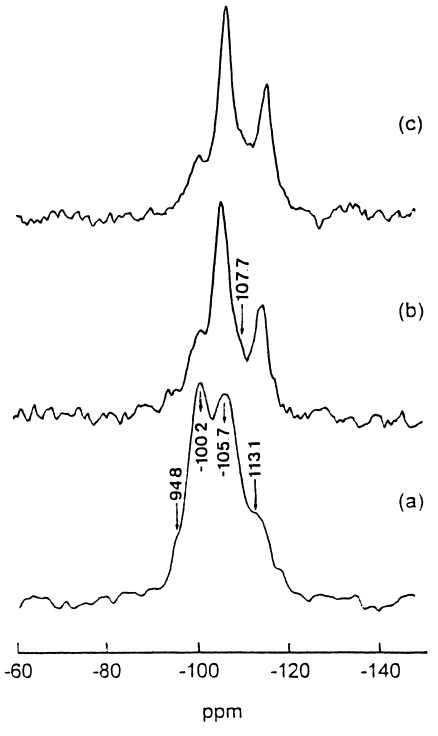

Fig. 3. ^{29}Si MAS NMR spectra of (a) H-omega, (b) $OMSA_{600,2}$ and (c) $OMSA_{700,2}$.

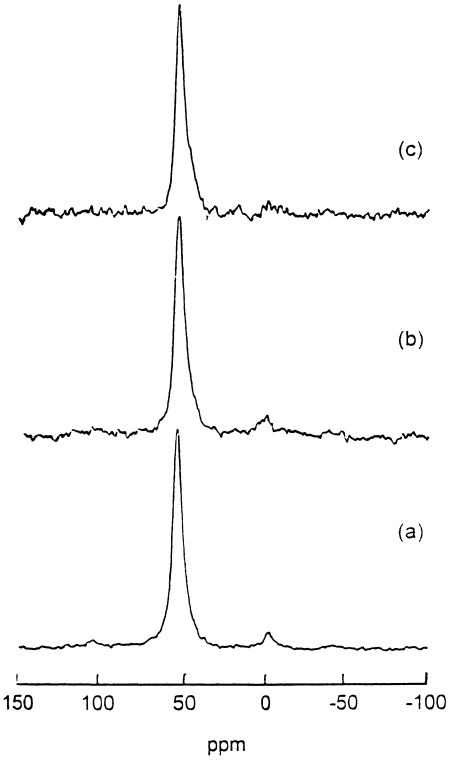

Fig. 4. ^{27}Al MAS NMR spectra of (a) H-MOR, (b) $MSA_{500,2}$, and (c) $MSA_{600,2}$.

[17]. It is clearly seen that nonstructural aluminum species were completely removed by acid leaching treatment.

In the case of H-omega, two broad peaks were observed: one at 55 and the other at 0 ppm. As observed in H-MOR, the peaks at 55 and 0 ppm are assigned to structural, tetrahedral aluminum and nonstructural, octahedral aluminum, respectively. Parent H-omega was observed to have a large amount of octahedral aluminum species. For the dealuminated samples, a new peak appeared near 30 ppm in addition to the peaks at 55 and 0 ppm. This peak is generally assigned to pentacoordinated nonstructural aluminum oxide [18]. Therefore, it is suggested that line broadening by dealumination, as noticed in the left peak of Fig. 5, may be due to the structural disorder, which is in accordance with the XRD result. Even after acid leaching, a relatively large amount of nonstructural aluminum species still remained in the pore. This result implies that some of the aluminum species extracted by steam treatment may be located in the pore such as gmelinite cage or 8-MR channel, so they could be hardly removed.

3.1.4. FT-IR of mordenite in the framework region

The infrared spectra of H-MOR and of its dealuminated samples in the region of 1400–400 cm^{-1} are presented in Fig. 6. According to the previous studies [19,20], the infrared bands at 730–720 and 620 cm^{-1} correspond to the isolated AlO_4 tetrahedra and alternating SiO_4 and AlO_4 tetrahedra in single 4-rings (S4R), respectively, and the band at 1225 cm^{-1} is assigned to the asymmetric Al–O vibration band of single 5-rings (S5R). With the degree of dealumination, intensities of the bands at 730–720 and 620 cm^{-1} decreased more significantly than that of the band at 1225 cm^{-1}. This indicates that aluminum species in S4R were removed preferentially by dealumination. Dealumination also brought about the decrease in band intensity near 956 cm^{-1}, assigned to Si–O

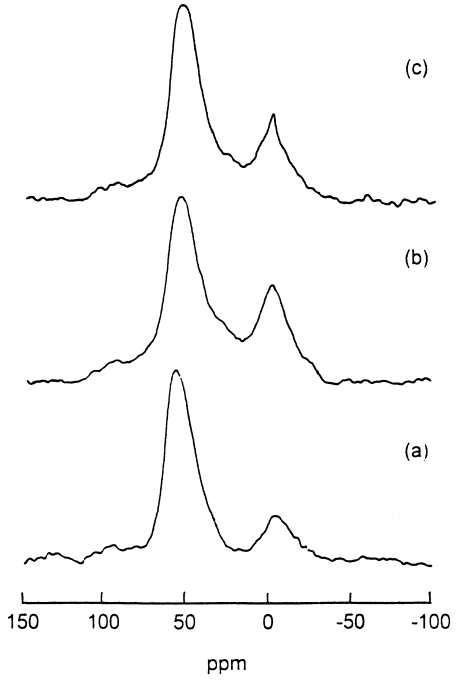

Fig. 5. ^{27}Al MAS NMR spectra of (a) H-omega, (b) $OMSA_{600,2}$ and (c) $OMSA_{700,2}$.

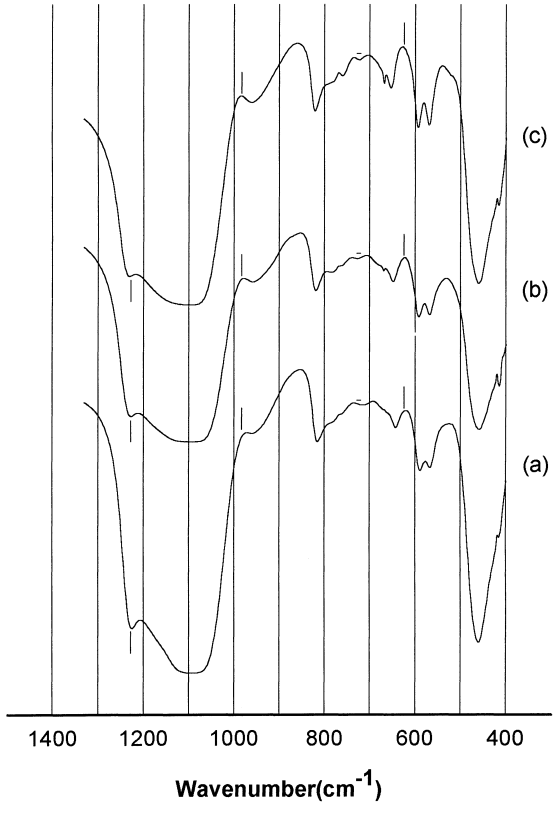

Fig. 6. FT-IR spectra in the framework region of (a) H-MOR, (b) $MSA_{500,2}$, and (c) $MSA_{600,2}$.

stretching vibration [13]. This implies that some hydroxyl nests were formed.

3.1.5. Ammonia TPD

The amount of acid sites measured by ammonia TPD are given in Table 2. Low temperature peak is mainly due to the weakly adsorbed ammonia on weak acid sites or nonacidic sites, whereas high temperature peak is related to desorption of ammonia from strong acid sites. The amount of strong acid sites increased in the order of H-beta, H-MOR and H-omega as shown in Table 2.

Table 2
Acidity of parent catalysts probed by ammonia

Catalysts	NH_3 desorbed (mmol/g-cat)	
	LT-peak[a] (T_m[c],°C)	HT-peak[b] (T_m,°C)
H-beta(12.5)	0.66 (200)	0.46 (320)
H-MOR	0.36 (230)	0.78 (700)
H-omega	0.76 (225)	1.84 (710)

[a] Ammonia desorbed at low temperature.
[b] Ammonia desorbed at high temperature.
[c] Maximum desorption temperature.

3.1.6. In situ FT-IR studies

Infrared spectra of pyridine adsorbed on parent zeolites in the region of ring vibrations of pyridinium ions are presented in Fig. 7. The band at 1540 cm^{-1} is assigned to pyridinium ions formed on Brønsted acid sites and that around 1450 cm^{-1} is due to pyridine coordinated to Lewis acid sites [20,21]. The intensity of the band at 1540 cm^{-1} corresponding to Brønsted acid sites was in the order H-MOR≈H-beta≫H-omega. This result is quite different from that of ammonia TPD (cf. Table 2). The molecular size of ammonia (kinetic diameter∼2.6 Å) is small enough to have access to almost all the acid sites in the microporous zeolites, but pyridine with kinetic diameter of

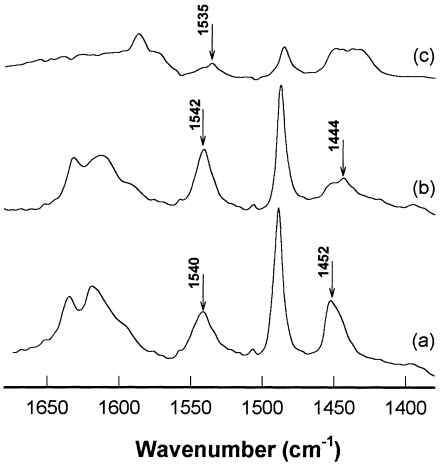

Fig. 7. FT-IR spectra of pyridine chemisorbed zeolites: (a) H-beta(12.5), (b) H-MOR, and (c) H-omega.

about 5.85 Å may not have access to the acid sites in relatively small pores.

Infrared spectra in the hydroxyl region of the samples are presented in Figs. 8–10. All the spectra show two main bands near the frequencies of 3600 and 3700 cm^{-1}, which correspond to the framework Si–OH–Al (acidic hydroxyl group) and the terminal (or external) silanols, respectively [21]. The broad bands at 3200–3100 and 3100–2950 cm^{-1} are due to pyridine ring stretching and ν(C–H) stretching, respectively. As shown in these figures, the bands for acidic hydroxyl groups of parent zeolites appeared at lower wave number in the order H-beta (3600 cm^{-1}), H-omega (3586 cm^{-1}) and H-MOR (3585 cm^{-1}). This result suggests that the strength of Brønsted acid sites is in the order H-MOR>H-omega≫H-beta.

The spectrum of H-beta shows a relatively small portion of acidic hydroxyl groups (3600 cm^{-1}). As mentioned above, the intense band at 3731 cm^{-1} represents terminal silanols. The broad band at about 3670 cm^{-1} is suggested to appear by two different groups [21]. One is Al–OH group with different chemical bonds from Si–OH–Al of 3600 cm^{-1} and the other is terminal silanol, expected at 3731 cm^{-1}, but lowered due to proton interaction. After pyridine chemisorption, the band for acidic hydroxyl groups disappeared almost completely and new bands in the range 3400–2950 cm^{-1} assigned to the bands of adsorbed pyridine appeared. This implies that nearly

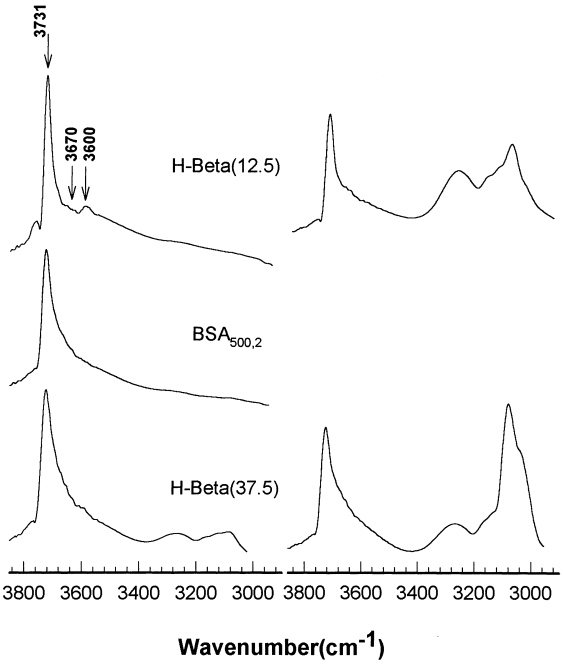

Fig. 8. FT-IR spectra in the hydroxyl region of H-beta(12.5), H-beta(37.5) and $BSA_{500,2}$ before (left) and after (right) pyridine chemisorption.

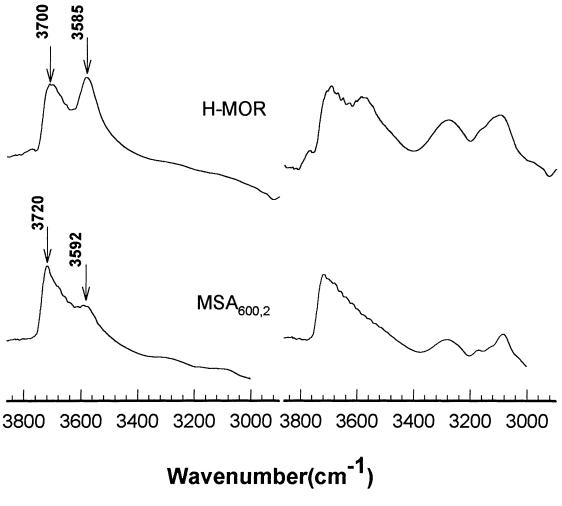

Fig. 9. FT-IR spectra in the hydroxyl region of H-MOR and $MSA_{600,2}$ before (left) and after (right) pyridine chemisorption.

all the Brønsted acid sites of H-beta were saturated with pyridine. The amount of acidic hydroxyl groups

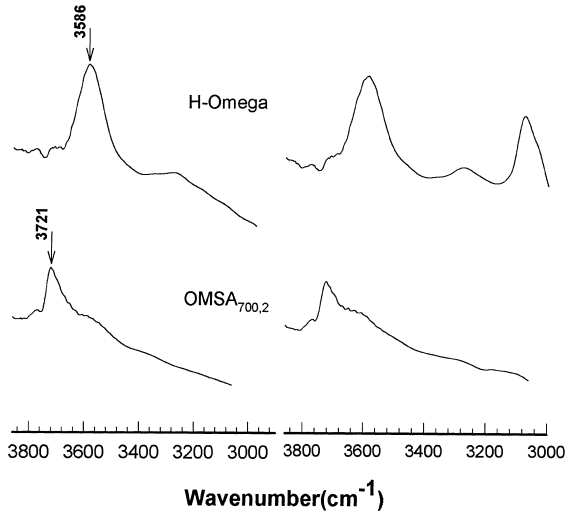

Fig. 10. FT-IR spectra in the hydroxyl region of H-omega and $OMSA_{700,2}$ before (left) and after (right) pyridine chemisorption.

decreased with Si/Al ratio, and the same result was obtained after dealumination.

H-MOR was observed to have a considerable amount of acidic hydroxyl groups (3585 cm^{-1}) in the structure as shown in Fig. 9. After pyridine chemisorption, a large portion of acidic hydroxyl groups remained unsaturated with pyridine. This indicates that a large number of acid sites in H-MOR are located in 8-MR channels and pyridine cannot have access to these acid sites. The peak intensity of acidic hydroxyl groups decreased substantially by dealumination, but most of acidic hydroxyl groups of $MSA_{600,2}$ were saturated with pyridine in contrast to the case of parent H-MOR.

As shown in Fig. 10, OH groups of H-omega were mainly in the form of acidic hydroxyl groups (3586 cm^{-1}), and indeed a relatively large amount of acidic hydroxyl groups were observed because of the low Si/Al ratio (=5.6) of H-omega. The peak intensity of acidic hydroxyl groups was almost unchanged after pyridine chemisorption. This implies that most of Brønsted acid sites of H-omega are located in 8-MR channels or in gmelinite cages to which pyridine cannot have access. After dealumination, acidic hydroxyl groups decreased while silanol groups (3721 cm^{-1}) increased significantly unlike the cases of H-beta and H-MOR. This result indicates that aluminum vacant sites created by framework dealumination were not replaced by silicon atoms and remained as structural defects such as hydroxyl nest in dealuminated samples.

3.2. Catalytic performance

In our previous study of H-beta for transalkylation of toluene and 1,2,4-TMB, maximum yield of xylene isomers was obtained at 400°C with mixture of toluene and 1,2,4-TMB of molar ratio 1 [22]. These conditions were adopted in all the reaction experiments. Three different reactions, disproportionation of toluene and of 1,2,4-TMB, and transalkylation between toluene and 1,2,4-TMB, can yield xylenes. Results of reaction experiments over various catalysts including the product distributions are given in Table 3.

Among the parent zeolites, both H-beta and H-MOR showed high yield of xylene isomers but the yield was very low over H-omega as shown in Fig. 11. According to the results of ammonia TPD, the Brønsted acidity of parent zeolites increases in the order of H-beta, H-MOR and H-omega. From the in situ pyridine FT-IR results, however, it was noticed that a large number of acid sites in H-MOR and H-omega were present in small pores or cages to which pyridine could not have access. For this reason, the Brønsted acidity probed by pyridine was quite

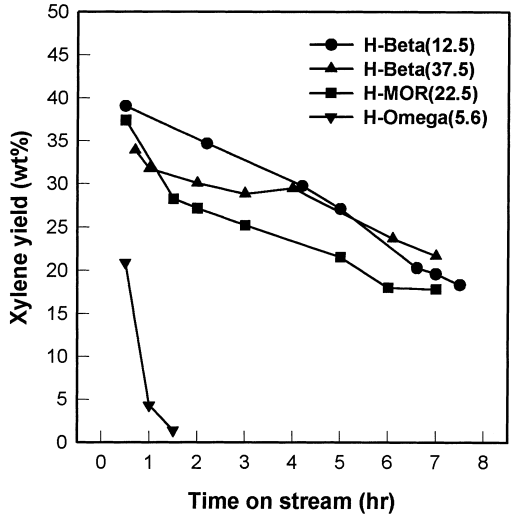

Fig. 11. Xylene yield as a function of the time on stream over parent zeolites.

Table 3
Product distributions from the transalkylation of toluene and 1,2,4-trimethylbenzene over various catalysts at reaction time of 3 h

Catalysts	Mordenite		Zeolite beta		Zeolite omega	
	H-MOR	$MSA_{600,2}$	H-beta(12.5)	$BSA_{500,2}$	H-omega[a]	$OMSA_{700,4}$
Product distribution (wt%)						
Benzene	0.9	1.6	0.7	0.4	0.1	1.1
Toluene	29.5	24.7	26.9	35.9	43.0	29.0
Xylene						
Para+meta	19.3	29.2	23.4	16.6	0.95	21.3
Ortho-	5.8	8.6	7.1	4.9	0.4	22.4
TMB						
1,3,5-	10.7	8.4	10.2	10.3	2.8	9.0
1,2,4-	25.7	20.3	24.0	23.9	37.6	26.1
1,2,3-	3.7	2.8	3.3	3.2	1.7	3.3
TeMB[b]						
1,2,4,5-	1.5	1.6	1.8	1.7	0.2	1.3
1,2,3,5-	2.0	2.0	2.2	2.2	0.2	1.6
1,2,3,4-	0.5	0.4	0.5	0.5	—	0.3
Conversion (wt%)						
Toluene conv.	40.9	43.8	39.4	18.3	2.0	34.0
TMB conv.	48.4	63.7	56.8	57.2	32	53.1
Xylene yield (wt%)	25.1	37.9	30.5	21.4	1.3	27.7

[a]Reaction time: 1.5 h.
[b]Tetramethylbenzene.

different from that probed by ammonia to be in the order H-MOR≈H-beta≫H-omega. Acid sites inaccessible to pyridine practically could not serve as adsorption sites for relatively large molecules such as toluene and 1,2,4-TMB. It is evident that the low catalytic activity of H-omega was caused by the low acidity probed by pyridine. Over the three parent zeolites, the order of activities are in accordance with the order of acidities probed by pyridine.

Concerning the stability of catalysts, H-beta gave rise to the best catalytic stability. H-MOR and H-omega were deactivated rapidly with the reaction time. Mordenite and zeolite omega possess 12-MR pore openings with unidimensional channels [14,15], whereas zeolite beta has three-dimensional interconnecting channel systems composed of linear channels and tortuous channels formed by the interaction of two linear channels [23]. Owing to this structural advantage, H-beta appears to be less affected by coke formation than H-MOR and H-omega.

As shown in Figs. 12–14, the stability of the parent zeolites was significantly enhanced after dealumination by steam treatment followed by acid leaching. As

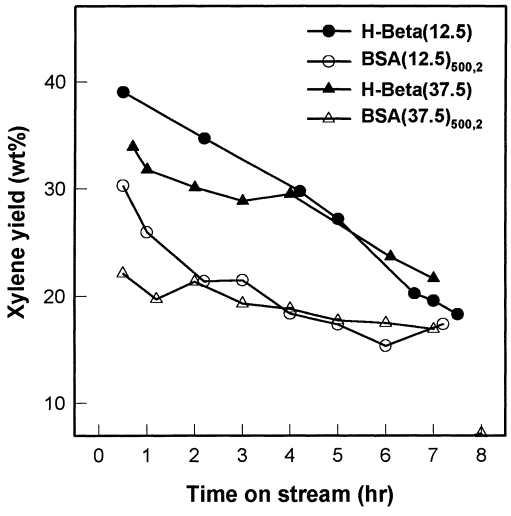

Fig. 12. Xylene yield as a function of the time on stream over H-beta and BSA series.

observed from the ^{29}Si MAS NMR spectra and IR spectra in the OH stretching region, steam and acid treatment caused significant framework dealumina-

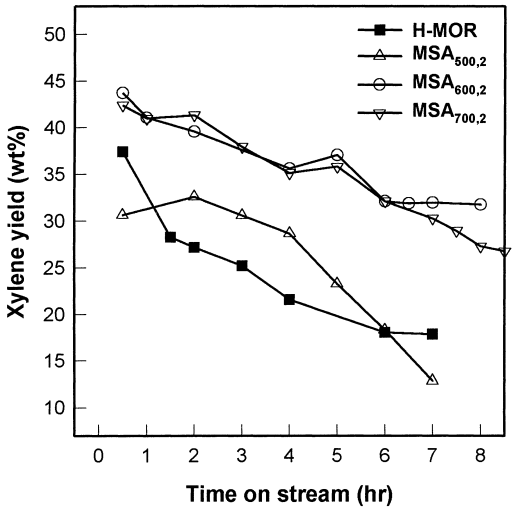

Fig. 13. Xylene yield as a function of the time on stream over H-MOR and MSA series.

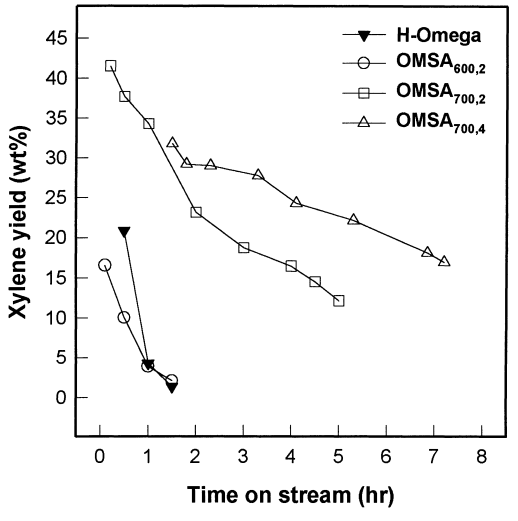

Fig. 14. Xylene yield as a function of the time on stream over H-omega and OMSA series.

tion. It is generally believed that after steam and acid treatment, aluminum sites become more spatially distributed. Therefore, coke formation from the dual-site mechanism [24] can be reduced.

As noticed in Fig. 12, the yield of xylene isomers over H-beta decreased after dealumination. This is mainly due to the reduction of the number of acid sites. However, dealuminated H-MOR and H-omega showed higher activity than parent zeolites in spite of the decrease in total acid sites. According to the mid-infrared spectra, MSA has more open structure by the partial destruction of S4R around 12-MR channel and thus the acid sites in side pockets or 8-MR channels become exposed to the main channel of 12-MR. These acid sites exposed to the main channel can serve as new adsorption sites for toluene and 1,2,4-TMB. In addition, more open structure of MSA would facilitate the diffusion of 1,2,4-TMB. This is supported by the results given in Table 3, in which it is noticed that toluene conversion was only slightly increased over $MSA_{600,2}$ whereas the conversion of 1,2,4-TMB considerably increased from 48.4% for H-MOR to 63.7% for $MSA_{600,2}$. This means that the higher yield of xylene isomers over $MSA_{600,2}$ is mainly attributed to the increase of reactivity of 1,2,4-TMB. The two features described above are understood to compensate for the loss of total acid sites and give rise to the high activity.

Most of acid sites in H-omega are present in S4R of gmelinite cages as one can see from the results of ^{29}Si MAS NMR and in situ pyridine FT-IR analyses. This is why the activity of parent H-omega was found to be very low. After steam and acid treatment, the pore structure became more open by virtue of the destruction of 8-MR channels or gmelinite cages during dealumination. This gave rise to the reduction of steric hindrance and thus the activity was enhanced. However, dealuminated H-omega turned out to be deactivated more rapidly than dealuminated H-beta and H-MOR.

4. Conclusions

Transalkylation of toluene and 1,2,4-trimethylbenzene has been studied over H-beta, H-MOR and H-omega, respectively, and also over their dealuminated samples which were treated by steam and dilute acid solution. In the case of the parent zeolites, it was observed that the acidities of H-omega and H-MOR were very high compared to that of H-beta. However, a large amount of Brønsted acid sites in H-omega and H-MOR turned out to be located in small pores and cages to which larger molecules such as pyridine and reactants including toluene and trimethylbenzene could not have access.

Among the parent zeolites, H-MOR and H-beta showed high activity and stability compared to H-omega for transalkylation reaction. Over dealuminated samples, the activity was found to be in the order H-MOR>H-omega≈H-beta unlike over the parent zeolites. After dealumination, both the catalytic activity and stability of H-MOR and H-omega were substantially improved while the activity of H-beta was decreased due to the loss of acid sites by dealumination. According to the results from ^{29}Si, ^{27}Al MAS NMR and mid-infrared spectra, it is evident that aluminum species in 4-ring near the 12-MR in H-MOR and H-omega are removed preferentially by dealumination to give more open structure. These structural changes are believed to compensate for the loss of total acid sites and give rise to the enhanced activity and stability of H-MOR and H-omega.

On the other hand, the nonframework aluminum species in H-omega could be hardly removed because they were located in gmelinite cages or 8-MR channels, whereas those in H-MOR were completely removed. Therefore, the activity remained low in case of H-omega compared to the case of dealuminated H-MOR. Furthermore, dealuminated H-omega was deactivated rather rapidly.

In conclusion, H-MOR could be a potential acid catalyst for transalkylation of toluene and 1,2,4-trimethylbenzene if H-MOR is subjected to precautious dealumination by steaming and acid leaching.

References

[1] J. Das, Y.S. Bhat, A.B. Halgeri, Catal. Lett. 23 (1994) 161.
[2] J.C. Wu, L.J. Leu, Appl. Catal. 7 (1983) 283.
[3] K.J. Chao, L.J. Leu, Zeolites 9 (1989) 193.
[4] I. Wang, T.C. Tsai, S.T. Huang, Ink. Eng. Chem. Res. 29 (1990) 2005.
[5] E. Dumitriu, V. Hulea, S. Kaliaguine, M.M. Huang, Appl. Catal. 135 (1996) 57.
[6] N.R. Meshram, S.B. Kulkarni, P. Ratnasamy, J. Chem. Tech. Biotechnol. A 34 (1984) 119.
[7] N.J. Topsøe, F. Joensen, E.G. Derouane, J. Catal. 110 (1988) 404.
[8] T.C. Tsai, H.Y. Kung, S.T. Yu, C.T. Chen, Appl. Catal. 50 (1989) 1.
[9] T.C. Tsai, I. Wang, Appl. Catal. 77 (1991) 209.
[10] E.V. Sobrinho, D. Cardoso, E. Falabella S-Aguiar, J.G. Silva, Appl. Catal. A. 127 (1995) 157.
[11] S. Nicolas, P. Massiani, M. Vera Pacheco, F. Fajula, F. Figueras, Stud. Surf. Sci. Chem. 37 (1988) 115.
[12] J.T. Miller, P.D. Hopkins, G.J. Meyers, J. Catal. 138 (1992) 115.
[13] P.C. van Geem, K.F.M.G.J. Scholle, G.P.M. van der Veid, J. Phys. Chem. 92 (1988) 1585.
[14] J. Datka, A. Kubacka, Zeolites 17 (1996) 428.
[15] E. Galli, Cryst. Struct. Commun. 3 (1974) 339.
[16] P. Massiani, B. Chauvin, F. Fajula, F. Figueras, Appl. Catal. 42 (1988) 105.
[17] J. Klinowski, J.M. Thomas, C.A. Fyfe, G.C. Gobbi, Nature (London) 296 (1982) 533.
[18] J.P. Gilson, G.C. Edwards, A.W. Peters, K. Rajagopalan, R.F. Wormsbecher, T.G. Roberie, M.P. Shatlock, J. Chem. Soc., Chem. Commun. (1987) 91.
[19] B.H. Ha, J. Guidot, D. Barthomeuf, J. Chem. Soc. Faraday Trans. 1 75 (1979) 1245.
[20] G. Coudurier, C. Naccache, J.C. Vedrine, J. Chem. Soc., Chem. Commun. (1982) 1413.
[21] M. Maache, A. Janin, J.C. Lavalley, Zeolites 13 (1993) 419.
[22] S.H. Park, J.K. Lee, H.-K. Rhee, Rep. Res. Inst. Eng. Sci., Seoul National University 16(1) (1996) 65.
[23] J.B. Higgins, R.B. LaPierre, J.L. Schlenker, A.C. Rohrman, J.D. Wood, G.T. Kerr, W.J. Rohrbaugh, Zeolites 8 (1988) 446.
[24] B.C. Gates, J.R. Katzer, G.C.A. Schmit, The Chemistry of Catalytic Processes, Academic Press, New York, 1977.